Citation: CPT Pharmacometrics Syst. Pharmacol. (2017) 6, 823–832; doi:10.1002/psp4.12259


ORIGINAL ARTICLE

# Pharmacokinetics and Pharmacodynamics of Meloxicam in East Asian Populations: The Role of Ethnicity on Drug Response

Takahiko Aoyama[1], Yoshimasa Ishida[1,2], Masato Kaneko[1,3], Aoi Miyamoto[1], Yoshiro Saito[4], Masahiro Tohkin[5,6], Shinichi Kawai[7] and Yoshiaki Matsumoto[1]*

**We aimed to reanalyze the differences in the pharmacokinetics (PKs) of meloxicam in East Asian populations based on a population approach using previously published data and to investigate the factors found in population PK analysis that affect the pharmacodynamics (PDs) of meloxicam. Population PK analysis was performed in 119 healthy male subjects (30 Japanese, 30 Chinese, 29 Korean, and 30 white) under strictly controlled trial conditions with regulated meals and a single lot of the drug. We found that *CYP2C9* genotype and lean body mass were statistically significant predictors of clearance and volume of distribution, respectively. A statistical significant difference in the PK parameters between ethnic groups could not be identified. Simulations using PK/PD models showed that *CYP2C9* genotype is the factor that affects the PDs of meloxicam. The genetic polymorphisms highlighted in this study would be beneficial for conducting clinical trials in East Asians with similar genetic backgrounds.**

*CPT Pharmacometrics Syst. Pharmacol.* (2017) **6**, 823–832; doi:10.1002/psp4.12259; published online 12 October 2017.

## Study Highlights

**WHAT IS THE CURRENT KNOWLEDGE ON THE TOPIC?**

☑ Clinical trial data have not been fully utilized among East Asian countries, such as Japan, China, and South Korea, because ethnic differences in PK and PD variables remain unclear.

**WHAT QUESTION DID THIS STUDY ADDRESS?**

☑ We re-analyzed the PK properties meloxicam in three East Asian populations and one white population using a population modeling approach with published data. Moreover, PK covariates that affect the PD properties of meloxicam were investigated in PK/PD modeling and simulation analyses.

**WHAT THIS STUDY ADDS TO OUR KNOWLEDGE**

☑ We showed that *CYP2C9* genotypes and LBM are statistically significant predictors of the CL and Vc of meloxicam, respectively, but that, of these predictors, only *CYP2C9* genotypes affect the PDs of meloxicam. In addition, no statistically significant differences in PK parameters were identified between the present East Asian populations.

**HOW MIGHT THIS CHANGE DRUG DISCOVERY, DEVELOPMENT, AND/OR THERAPEUTICS?**

☑ The roles of *CYP2C9* polymorphisms demonstrated herein may be applicable to future studies of ethnic differences, and the ensuing insights may facilitate clinical trials in East Asian populations with similar genetic backgrounds.

During recent decades, numbers of global clinical trials have increased because of the need for timely drug approval in multiple countries.[1] In these clinical trials, interethnic differences in pharmacokinetic (PK) and pharmacodynamic (PD) properties should be considered. Moreover, because interethnic differences in PK properties have been reported between East Asian and white populations, the clinical trial results of one group cannot be readily extrapolated to the other.[2–4] It also remains unclear whether interethnic differences in PK and PD properties of medications are present among East Asian populations, although East Asian clinical trials have been effective for some high prevalence diseases, such as gastric cancer.[5]

Thus, it may be necessary to clarify ethnic differences in PKs and PDs to facilitate the utilization of clinical trial data across East Asian countries, such as Japan, China, and South Korea. Accumulation of this information may also improve the planning of East Asian clinical trials by decreasing costs and shortening study durations. The factors associated with interethnic differences in the PKs of medications include intrinsic factors, such as genotype, and extrinsic factors, such as dietary patterns and coadministered medications. Therefore, clinical trials that are strictly controlled for these extrinsic factors could be used to evaluate interethnic differences in the PKs of drugs in terms of the associated intrinsic factors. To clarify and explain ethnic

[1]Laboratory of Clinical Pharmacokinetics, School of Pharmacy, Nihon University, Chiba, Japan; [2]Clinical Pharmacology Strategy, Japan Medical and Development, Bristol-Myers Squibb, Tokyo, Japan; [3]Clinical Sciences Japan, Bayer Yakuhin, Ltd, Osaka, Japan; [4]Biochemistry and Immunochemistry, National Institute of Health Science, Tokyo, Japan; [5]Division of Medicinal Safety Science, National Institute of Health Science, Tokyo, Japan; [6]Department of Regulatory Science, Graduate School of Pharmaceutical Sciences, Nagoya City University, Aichi, Japan; [7]Department of Inflammation and Pain Control Research, Toho University School of Medicine, Tokyo, Japan. *Correspondence: Y Matsumoto (matsumoto.yoshiaki@nihon-u.ac.jp)
Received 22 August 2017; accepted 5 October 2017; published online on 12 October 2017. doi:10.1002/psp4.12259

**Table 1** Demographic data

| | Ethnicity | | | |
|---|---|---|---|---|
| **Characteristics** | **Japanese** | **Chinese** | **Korean** | **White** |
| No. of subjects | 30 | 30 | 29 | 30 |
| Smoking history | 9 | 1 | 2 | 6 |
| Age, years | 24 (21–30) | 31 (23–34) | 24 (21–29) | 26 (21–35) |
| Weight, kg | 63.5 (52.1–84.5) | 67.0 (51.0–91.0) | 69.1 (56.3–84.4) | 74.5 (55.9–100) |
| BMI, $kg/m^2$ | 21.7 (18.6–29.1) | 23.5 (19.2–29.0) | 22.6 (19.2–26.3) | 24.6 (19.9–29.8) |
| BSA, $m^3$ | 1.75 (1.56–2.00) | 1.78 (1.53–2.08) | 1.86 (1.64–2.06) | 1.93 (1.62–2.30) |
| LBM, kg | 52.5 (44.5–62.9) | 54.0 (43.6–66.3) | 57.3 (47.6–65.2) | 59.8 (47.1–75.2) |
| Height, cm | 172 (161–180) | 168 (160–180) | 177 (168–186) | 177 (162–195) |
| eGFR, mL/min | 97.4 (74.1–138) | 120 (92.8–152) | 116 (98.9–151) | 121 (85.4–158) |
| ALB, g/dL | 4.5 (4.0–4.9) | 4.4 (4.0–5.0) | 4.4 (4.0–5.2) | 4.5 (3.9–4.9) |
| ALT, IU/L | 15 (8–38) | 16 (6–29) | 13 (3–38) | 19 (9–63) |
| AST, IU/L | 16 (12–25) | 20 (14–35) | 16 (11–31) | 20 (12–82) |
| DBIL, mg/dL | 0.2 (0.1–0.6) | 0.2 (0.1–0.5) | 0.3 (0.1–0.7) | 0.1 (0.0–0.27) |
| HDL, mg/dL | 52 (37–100) | 49 (29–69) | 51 (29–97) | 50 (30–78) |
| LDH, IU/L | 135 (106–189) | 120 (83–152) | 159 (130–469) | 133 (98–259) |
| LDL, mg/dL | 86 (53–177) | 105 (41–159) | 104 (59–130) | 88 (45–141) |
| TBIL, mg/dL | 1.0 (0.4–2.2) | 0.9 (0.5–1.6) | 1.2 (0.6–2.0) | 0.6 (0.3–2.1) |
| TG, mg/dL | 84 (46–384) | 108 (65–203) | 84 (46–172) | 105 (39–304) |
| TP, g/dL | 7.1 (6.2–7.7) | 7.8 (6.9–8.3) | 6.9 (6.3–8.6) | 6.9 (6.1–8.2) |
| GGT, IU/L | 20 (10–50) | 16 (11–34) | 15 (9–34) | 16 (6–58) |

Data are expressed as median (range).
ALB, serum albumin; ALT, alanine aminotransferase; AST, aspartate aminotransferase; BMI, body mass index; BSA, body surface area; DBIL, direct bilirubin; eGFR, estimated glomerular filtration rate; GGT, gamma-glutamyl transpeptidase; HDL, high-density lipoprotein cholesterol; LBM, lean body mass; LDH, lactate dehydrogenase; LDL, low-density lipoprotein cholesterol; TBIL, total bilirubin; TG, triglyceride; TP, total protein.

differences in PK parameters, Hasunuma *et al.*[6] investigated differences in exposure levels of moxifloxacin, simvastatin, and meloxicam among Japanese, Chinese, and South Korean healthy male subjects. In that research, data from a single lot of the drug was used; food calories, nutritional content, and hardness of the drinking water were matched; and plasma meloxicam concentrations were measured from a single site. However, no detailed ethnic evaluations of the PKs of meloxicam have been performed among East Asian populations using a population approach.

Meloxicam is a cyclooxygenase inhibitor commonly used to treat patients with pain due to rheumatoid arthritis[7] and surgery.[8] The dose proportionality between orally administered doses of 7.5–30 mg has been confirmed,[9] and the total clearance, volume of distribution, and absolute bioavailability have been reported to be 7.2 mL/min, 10.7 L, and 89% in healthy subjects, respectively. In addition, the terminal elimination half-life of meloxicam was 20 hours, and the plasma protein binding consistently reached 99.5% over the concentration range used in clinical practice.[10] Approximately 0.6% of the intravenously administered drug was excreted in the urine,[11] and meloxicam is primarily metabolized to its 5′-hydroxymethyl metabolite by cytochrome P450 2C9 (CYP2C9). Meloxicam enters enterohepatic and/or enteroenteric circulations, as indicated by increased meloxicam clearance after intravenous administration with cholestyramine coadministration.[10,12] Lehr *et al.*[13] also reported a population PK model of meloxicam that incorporates the enterohepatic circulation. The thromboxane $B_2$ ($TXB_2$) generation is commonly used as a biomarker of cyclooxygenase activity,[14–16] and it is a stable product of cyclooxygenase-mediated thromboxane $A_2$ catabolism. A sequential population PK/PD model of meloxicam was previously reported by Tegeder *et al.*,[17] who monitored cyclooxygenase inhibition according to decreased $TXB_2$ generation. Rohatagi *et al.*[18] also reported a relationship between serum $TXB_2$ contents and the incidence of gastroduodenal ulcers and erosions.

The study objective was to reanalyze differences in PKs of meloxicam among East Asian (Japanese, Chinese, and South Koreans) and white populations using population PK analyses of published clinical trial data. Accordingly, we investigated how factors found in population PK modeling affect PDs of meloxicam using PK/PD models and simulations. Understanding of the factors that affect $TXB_2$ generation after meloxicam administration may reveal useful biomarkers of meloxicam efficacy and safety in East Asian populations.

## METHODS

### Data source

*Population pharmacokinetic modeling.* Plasma meloxicam concentrations and clinical data from Hasunuma *et al.*[6] were used as the source of population PK modeling data. Subject characteristics are shown in **Table 1**. One hundred nineteen healthy male subjects (*CYP2C9* genotypes: Japanese, 26 subjects with **1/*1* and 4 subjects with **1/*3*; Chinese, 26 subjects with **1/*1*, 1 subject with **1/*2*, and 3 subjects with **1/*3*; Korean, 25 subjects with **1/*1* and 4 subjects with **1/*3*; and white, 20 subjects with **1/*1*, 5

subjects with **1/*2*, 1 subject with **2/*2*, and 4 subjects with **1/*3*) were administered single oral doses of meloxicam (7.5 mg).[6] Blood samples were collected before and at 1, 2, 3, 4, 5, 6, 8, 12, 24, 36, 48, 60, and 72 hours after drug administration, and plasma meloxicam concentrations were determined using liquid chromatography-tandem mass spectrometry.[6] The trial was registered in the UMIN Clinical Trials Registry system (UMIN000004173), and the population PK study was approved by the Ethics Committee of the School of Pharmacy, Nihon University.

*Pharmacokinetic/pharmacodynamic modeling.* Plasma meloxicam concentrations and the inhibition of $TXB_2$ generation were retrieved from the data of Bae *et al.*[14] and were used as source data for PK/PD modeling. Graphs of plasma meloxicam concentration-time data and percentage inhibition of $TXB_2$ generation relative to baseline levels were scanned, and all graphed data points were digitized using UN-SCAN-IT software (Silk Scientific, Orem, UT). These graphs represent the averaged data and are only separated by *CYP2C9*1/*1* or *CYP2C9*1/*13* genotypes. Demographic data (numbers or means ± SDs) for subjects of the *CYP2C9*1/*1* group includes 12 healthy Korean volunteers of age 23.2 ± 2.6 years and body weights of 71.8 ± 8.1 kg. The data for subjects in the *CYP2C9*1/*13* group includes 9 healthy Korean volunteers of age 24.4 ± 2.5 years and body weights of 70.7 ± 7.3 kg. Percent serum $TXB_2$ generation relative to basal values was calculated as the difference between 100% and the scanned percent inhibition of $TXB_2$ generation. Twenty-one healthy male volunteers carrying either *CYP2C9*1/*1* or *CYP2C9*1/*13* genotypes were administered single oral doses of meloxicam (15 mg).[14] In that report, blood samples for determinations of plasma meloxicam concentrations and $TXB_2$ generation were collected before and at 1, 2, 3, 4, 5, 6, 8, 10, 12, 24, 48, and 72 hours after the administration of meloxicam.[14] The SDs of plasma concentrations and percent inhibition of $TXB_2$ generation at 1–8 hours after administration were not digitized because the error bars were not recognized for all groups.

**Population pharmacokinetic modeling**

Population analyses were performed using NONMEM version 7.2,[19] PsN,[20] Wings for NONMEM (http://wfn.sourceforge.net/), and Xpose[21] software packages. Population PK parameters were estimated using first-order conditional estimations with interactions. Model selection was based on the objective function value (OFV) calculated by NONMEM, the relative SE of the parameter estimates, and model diagnosis plots.[22]

To describe plasma meloxicam concentration profiles during the absorption phase, several structural models were estimated using one-compartment or two-compartment models with first-order absorption, transit absorption, and zero-order and first-order parallel absorption with or without lag time. Additionally, to describe fluctuating plasma concentration profiles during the elimination phase, the enterohepatic circulation model[13] was tested. In these analyses, interindividual variability in PK parameters was assumed to follow log-normal distributions and was modeled using exponential functions, whereas residual variability was evaluated using a proportional error model and a combined additive plus proportional error model. Parameters with individual values between 0 and 1 were modeled as follows:

$$\mathrm{A}=\mathrm{Ln}\{\theta_F/(1-\theta_F)\} \quad (1)$$

$$\mathrm{F}_j=\exp\left(A+\eta_j^F\right)/\left(1+\exp\left(A+\eta_j^F\right)\right), \quad (2)$$

where $A$ is a temporary variable, $\theta_F$ corresponds with a typical value of a fraction in the j[th] individual, *Fj* corresponds with the estimated fraction of the j[th] individual, and $\eta_j^F$ represents normally distributed interindividual variability with a mean of zero and a variance of $\omega_F{}^2$.[23]

Potential covariates were investigated using stepwise forward addition and backward elimination with *P* values of 0.01 and 0.001, respectively. An ethnic difference was defined as the difference that is not explained by demographic data, including age, body size, renal function, smoking history, other clinical laboratory data, and *CYP2C9* genotypes. Potential covariates in the forward step were investigated step-by-step in the following order (i.e., at each step, the model with the lowest OFV was forwarded to the next step if it was statistically significant): age, body size index (body weight, body mass index, lean body mass (LBM) using the James formula,[24] and body surface area), renal function data (estimated glomerular filtration rate[25–27]), smoking history, other clinical laboratory data, *CYP2C9* genotypes, and ethnic differences. Relationships between parameters and tested covariates are shown in **Supplementary Table S1**.

Covariates were introduced into the model as either continuous or categorical functions. Continuous covariates were centered on the median value of the population and were modeled using the following power equation:

$$P_i = P_{pop}\cdot(covariate/median\ \ covariate)^{\theta}, \quad (3)$$

where $\theta$ is a covariate scale factor that describes the magnitude of the covariate-parameter relationships. Categorical covariates were modeled as follows:

$$P_i = P_{pop}\cdot(1+n\cdot\theta), \quad (4)$$

where *n* is an indicator variable (0/1), and *CYP2C9* polymorphisms were modeled as follows:

$$CLpop = CL_{*1/*1}\cdot(1+n_{*2}\cdot\theta_{*2}\ +n_{*3}\cdot\theta_{*3}), \quad (5)$$

where $CL_{pop}$ is the apparent clearance of meloxicam, CL**1/*1* is the total apparent clearance for subjects with the *CYP2C9*1/*1* genotype, and $n_{*x}$ *and* $\theta_{*x}$ are numbers of alleles and the fractional changes of $CL_{*1/*1}$ attributable to respective genes.[28–30] Ethnic differences were modeled using the following expression:

$$P_{pop} = P_{ja}\cdot(1+n_{ch}\cdot\theta_{ch}\ +n_{ko}\cdot\theta_{ko}\ +n_{ca}\cdot\theta_{ca}), \quad (6)$$

where $P_{pop}$ is the PK parameter, $P_{ja}$ is the PK parameter for Japanese patients, *n* and $\theta$ are indicator variables (0/1) representing fractional changes in PK parameters of

Chinese (*ch*), Korean (*ko*), and white (*ca*) subjects compared with those of Japanese subjects.

### Model qualification

Uncertainty in parameter estimates was assessed using bootstrapping, and resampling was performed 1,000 times and was stratified by the *CYP2C9* genotypes. Median values and 2.5th and 97.5th percentiles of parameter estimates from these analyses were compared with those of the final model. The performance of the final population PK model was evaluated using a prediction-corrected visual predictive check (pc-VPC),[22,31] which was generated by simulating 1,000 replicates of the study from the final models. For visual inspection, 95% confidence intervals for the 5th, 50th, and 95th percentiles of simulated concentrations at each time point are shown as areas, and 5th, 50th, and 95th percentiles of the observed data are represented as lines.

To compare predictions from the final population PK model with those from previously reported data, we simulated 1,000 individuals who were administrated meloxicam.[32] To compare the profiles reported by Bae *et al.*,[14] plasma concentration profiles were simulated after single-dose administration. In these computations, the *CYP2C9* genotype was set to **1/*1* and the LBMs of 1,000 individuals were generated using a parametric approach based on original datasets. Plasma concentration-time profiles after multiple administrations were also simulated and compared with those reported by the "interview form" of Morbic tablets (drug information media used in Japan).[33] The *CYP2C9* genotype distribution was generated at the same ratio as for the original dataset, and the LBMs of 1,000 individuals were parametrically derived from the original dataset.

### Pharmacokinetic/pharmacodynamic modeling

The PK parameters were estimated using the structure model that was selected by population PK analyses. Specifically, PD modeling was performed using a sequential approach using PD observations and PK predictions based on the PK model. The PK/PD model comprised the PK model and the indirect response model with input inhibition. On the basis of decreased $TXB_2$ generation because of the inhibition of cyclooxygenase by meloxicam, rates of change in percent serum $TXB_2$ generation relative to basal values were described by the following physiological indirect response model[34–36]:

$$\frac{dR}{dT} = k_{in} \cdot \left(1 - \frac{Cp^{\gamma}}{IC_{50}^{\gamma} + Cp^{\gamma}}\right) - k_{out} \cdot R \qquad (7)$$

where $R$ is percent serum $TXB_2$ generation relative to the basal value, $k_{in}$ is the zero-order rate constant for the increase in the percent serum $TXB_2$ generation of the basal value, $Cp$ is the plasma meloxicam concentration, $IC_{50}$ is the plasma meloxicam concentration that decreases $k_{in}$ by 50%, $k_{out}$ is the first-order rate constant for the decrease in percent serum $TXB_2$ generation of the basal value, and $\gamma$ is a sigmoidicity parameter. Under basal conditions, percent serum $TXB_2$ generation value was 100%, with $k_{in}$ set as $100^{*}k_{out}$.

### Simulation

To quantify the impact of covariates on clearance (CL) and volume of distribution in the central compartment (Vc) to PDs, the population mean of the final population PK model was used to simulate meloxicam steady-state concentrations at a dosing schedule of 7.5 mg once daily. The CL was calculated for *CYP2C9*1/*1*, **1/*2*, **1/*3*, **2/*2*, **2/*3*, and **3/*3* genotypes, and Vc was calculated at LBMs of 75.2, 55.0, and 43.6 kg, reflecting maximum, median, and minimum LBMs of the populations in the original dataset, respectively. Simulated meloxicam concentrations and PD parameter estimates from the PK/PD model were used to simulate steady-state effects of meloxicam. These simulations are deterministic and the time-weighted average percent serum $TXB_2$ generation over 24 hours relative to the basal value was used as a summary parameter to characterize time courses of each endpoint after meloxicam administration.

## RESULTS

### Population pharmacokinetic modeling

Concentration-time profiles of ethnic groups are shown in **Figure 1a**, and double logarithmic concentration-time profiles in the absorption phase of ethnic groups are shown in **Figure 1b**. The profiles of the subjects had convex downward curves and straight lines during the absorption phase, as observed in **Figure 1b**. Therefore, a one-compartment model with a transit absorption model,[37,38] and zero-order and first-order parallel absorption with lag time model[39] were tested. In the latter model, the estimated time (1.42 hours) for meloxicam to enter the central compartment according to the zero-order process was close to the estimated absorption lag time of 1.9 hours with the first-order rate process. However, because discontinuation of absorption between 1.42 and 1.9 hours is physiologically unlikely, the estimated time for the zero-order process was assumed equal to the absorption lag time even though the OFV was increased ($\Delta$OFV = 49.928; df = 1). Moreover, the OFV for the parallel absorption model was lower than that of the transit absorption model ($\Delta$OFV = 249.780; df = 2) and the first-order absorption with the lag time model ($\Delta$OFV = 388.343; df = 2). The OFV for the two-compartment model with zero-order and first-order parallel absorption with the lag time model was lower than that of the one-compartment model ($\Delta$OFV = 129.673; df = 2). Tests of the enterohepatic circulation model[13] were hampered by convergence. The OFV for combined additive and proportional model was the same as that for the proportional error model, and the SD of additive error in the residual variability was 0.00546 ng/mL. Thus, residual variability was modeled using a proportional error model. We concluded that the two-compartment model with the parallel absorption model described the data adequately, and we used this for the final structure model (**Figure 2**). Interindividual variability was estimated reliably for apparent CL, apparent Vc, the first-order absorption rate constant ($k_a$), and the dose fraction absorbed by zero-order absorption (F), which showed a correlation between $k_a$ and F.

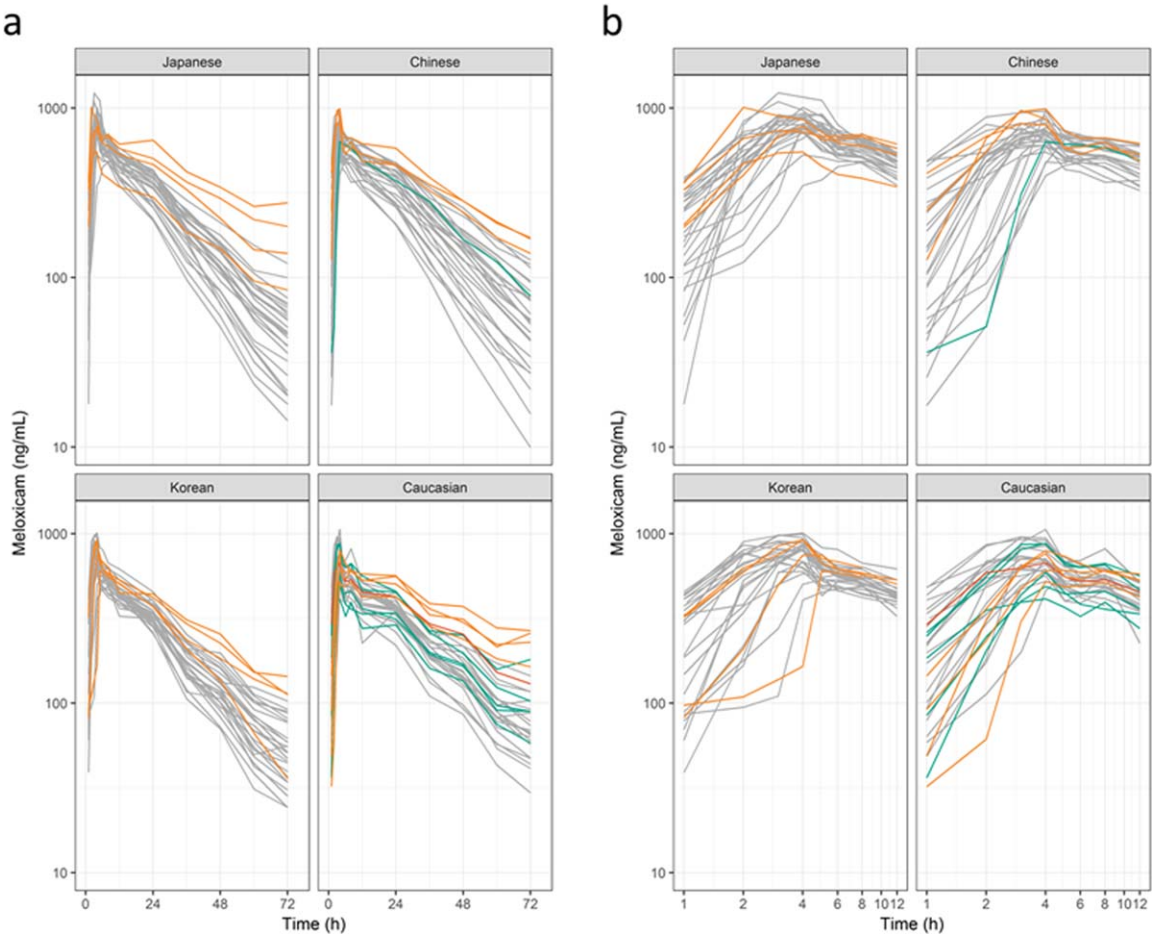


**Figure 1** Plasma concentration-time profiles of meloxicam for (**a**) single and (**b**) double logarithmic plots. Individuals are represented by lines. Colors represent *CYP2C9* genotypes; gray line, **1/*1*; green line, **1/*2*; orange line, **1/*3*; and red line, **2/*2*.

In the covariate model summarized in **Supplementary Table S2**, the full model included LBM and serum albumin as covariates for Vc, and *CYP2C9* genotypes as covariates for CL after the forward step. In the backward step, exclusion of *CYP2C9* genotypes from CL ($\Delta$OFV = 57.854; df = 2; $P < 0.001$) and LBM from Vc ($\Delta$OFV = 41.335; df = 1; $P < 0.001$) caused statistically significant increases in OFV. No statistically significant ethnic differences were identified in PK parameters. The bootstrapping results and final population PK parameter estimates of meloxicam are shown for the final model in **Table 2**. The model predicted CL for meloxicam was decreased by 15%, 29%, 40%, 55%, and 80% in subjects with *CYP2C9*1/*2*, **2/*2*, **1/*3*, **2/*3*, and **3/*3* genotypes, respectively, compared with that in subjects with the *CYP2C9*1/*1* genotype. We also stratified concentration-time profiles by LBM (**Figure 3**) and present model diagnosis plots in **Supplementary Figure S1**.

The present pc-VPC results (**Supplementary Figure S2a**) were stratified by ethnicity and *CYP2C9* genotypes and are presented in **Supplementary Figures S3 and S4**, respectively. In the pc-VPC, the percentile intervals describing prediction-corrected observations were mostly within the 95% confidence intervals of percentile intervals for the simulated concentrations. **Supplementary Figures S2b and S2c** show the reported concentrations for single-dosing and multiple-dosing strategies, respectively, and the results of the simulation are compared with those of previous studies,[14,33] which provide external validation of our model. The pc-VPC of the final model indicates the absence of model misspecification and good simulation properties. The external validation indicates that the model seems to systemically underpredict the external data.

### Pharmacokinetic/pharmacodynamic modeling

The PK/PD model (**Figure 2**) and the PK/PD parameter estimates and their SEs (**Table 3**) were estimated using the same structure model as selected for the population PK analysis. Time courses of observed and predicted meloxicam concentrations and percent serum $TXB_2$ generation relative to basal values are shown with residual plots in **Figure 3**. Reasonable agreement was demonstrated between observed and predicted effects of meloxicam, as there is a tendency for bias at later time points for each group.

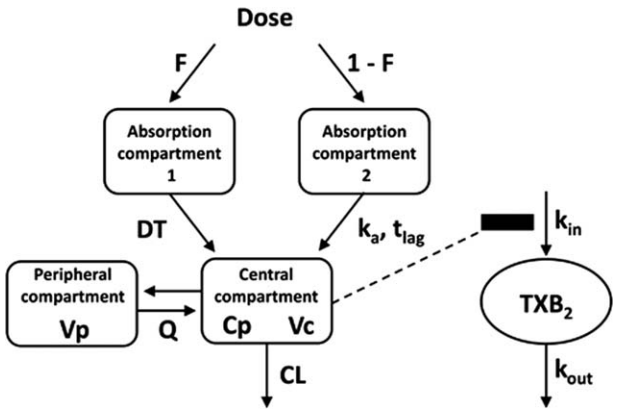


**Figure 2** Pharmacokinetic/pharmacodynamic model for meloxicam. Absorption phase profiles are described by zero-order absorption and first-order absorption with the lag time model. CL, apparent clearance; Cp, plasma meloxicam concentrations; DT, duration of meloxicam entry into the central compartment from the absorption compartment 1 by zero-order rate; F, fraction of the dose absorbed through the zero-order absorption process; $k_a$ and $t_{lag}$, first-order rate constant and lag time, respectively; $k_{in}$, zero-order rate constant for increases in percent serum thromboxane $B_2$ ($TXB_2$) generation relative to basal values; $k_{out}$, first-order rate constant for decreases in percent serum $TXB_2$ generation; Q, apparent intercompartmental clearance; Vc, apparent volume of distribution in the central compartment; Vp, apparent volume of distribution in the peripheral compartment.

### Simulation

**Figure 4** shows the relationships between changes in covariates and the effects of meloxicam. The time-weighted average percentage serum $TXB_2$ generation values for 24 hours at steady state in typical subjects with *CYP2C9*1/*1*, **1/*2*, **1/*3*, **2/*2*, **2/*3*, or **3/*3* genotypes were 60.5%, 57.6%, 51.0%, 54.0%, 45.7%, or 31.8%, respectively, and corresponding LBMs were 75.2, 55.0, or 43.6 kg and 60.3%, 60.5%, or 60.7%, respectively. The simulated time-weighted average percentage serum $TXB_2$ generation value of a typical subject with the *CYP2C9*3/*3* genotype was 0.53-fold that of a typical subject with the *CYP2C9*1/*1* genotype.

## DISCUSSION

Quantitative investigations of differences in PK and PD properties of medications among Japanese, Chinese, and South Korean populations may provide fundamental information for improving the efficacy and safety of medications and the efficiency of drug development. Therefore, we investigated the ethnic differences in the PKs of meloxicam using a population modeling approach based on data obtained from the trial under strict conditions.

In this study, the structural model of meloxicam was characterized by a two-compartment model with zero-order and first-order parallel absorption with lag time. Lehr *et al.*[13] previously developed an enterohepatic circulation model controlled by a sine function for meloxicam PKs following intravenous administration. In addition, Hasunuma *et al.*[6] showed that the second peak or delayed absorption in the PK profile of meloxicam is observed at around 8 hours after administration. Herein, we tested the enterohepatic circulation model[13] to describe this phenomenon, but were

**Table 2** Parameter estimates and bootstrap confidence intervals for the population pharmacokinetic model

| | Original dataset | | Bootstrap result | |
|---|---|---|---|---|
| **Parameter** | **Estimate (±1.96 × SE)** | | **Median (95% CI)** | |
| CL (L/h) | 0.391 | (0.375 to 0.407) | 0.390 | (0.375 to 0.407) |
| *CYP2C9 *2* on CL | −0.147 | (−0.234 to −0.0604) | −0.147 | (−0.215 to −0.0410) |
| *CYP2C9 *3* on CL | −0.400 | (−0.488 to −0.312) | −0.400 | (−0.483 to −0.301) |
| Vc (L) | 7.79 | (7.24 to 8.34) | 7.80 | (7.01 to 8.35) |
| LBM on Vd | 1.05 | (0.695 to 1.40) | 1.06 | (0.746 to 1.41) |
| Q (L/h) | 1.24 | (0.948 to 1.53) | 1.24 | (1.00 to 1.68) |
| Vp (L) | 2.73 | (2.20 to 3.26) | 2.72 | (2.22 to 3.49) |
| Ka (/h) | 2.00 | (1.38 to 2.62) | 2.05 | (1.44 to 2.84) |
| DT (h) | 1.91 | (1.86 to 1.96) | 1.91 | (1.83 to 1.94) |
| F | 0.425 | (0.367 to 0.483) | 0.423 | (0.364 to 0.481) |
| $\omega_{CL}$ (CV%) | 21.3 | (18.4 to 23.9) | 21.0 | (18.2 to 23.5) |
| $\omega_{Vd}$ (CV%) | 17.2 | (13.4 to 20.3) | 17.1 | (14.0 to 20.0) |
| $\omega_{Ka}$ (CV%) | 131 | (68.1 to 201) | 130 | (81.5 to 193) |
| $\omega^2_F$ | 2.03 | (1.46 to 2.60) | 2.00 | (1.45 to 2.62) |
| $\omega_{Ka}$-$\omega_F$ | 0.243 | (0.0269 to 0.459) | 0.262 | (0.0421 to 0.482) |
| $\sigma$ (CV%) | 12.3 | (11.3 to 13.2) | 12.3 | (11.4 to 13.2) |

CI, confidence interval; CL, apparent clearance; $CL_{pop}$, population mean of apparent clearance; DT, duration of meloxicam entry into the central compartment from the absorption compartment by zero-order rate; F, fraction of the dose absorbed through the zero-order absorption process; Ka, first-order absorption rate constant; LBM, lean body mass; $n_{*2}$, number of *CYP2C9*2* alleles; $n_{*3}$, number of *CYP2C9*3* alleles; Q, apparent intercompartmental clearance; $t_{lag}$, absorption lag time for meloxicam entry into the central compartment from the absorption compartment with the first-order rate; Vc, apparent volume of distribution in the central compartment; $Vc_{pop}$, population mean of apparent volume of distribution in the central compartment; Vp, apparent volume of distribution in the peripheral compartment; $\omega_{CL}$, interindividual variability of CL; $\omega^2_F$, interindividual variability of F; $\omega_{Ka}$, interindividual variability of Ka; $\omega_{Ka}$-$\omega_F$, correlation coefficient between interindividual variability of Ka and that of F; $\omega_{Vd}$, interindividual variability of Vd; $\sigma$, residual variability.
DT and $t_{lag}$ were set to the same value. Eta-shrinkage: CL, 1.89%; Vc, 8.81%; Ka, 12.0%; F, 6.30%. Epsilon-shrinkage: 13.7%. Calculations: $t_{lag}$ = DT (h). The final population pharmacokinetic equation was $CL_{pop}(L/h) = 0.391 \cdot (1 - n_{*2} \cdot 0.147 - n_{*3} \cdot 0.400)$, where $Vc_{pop}(L) = 7.79 \cdot (LBM/55.0)^{1.05}$.

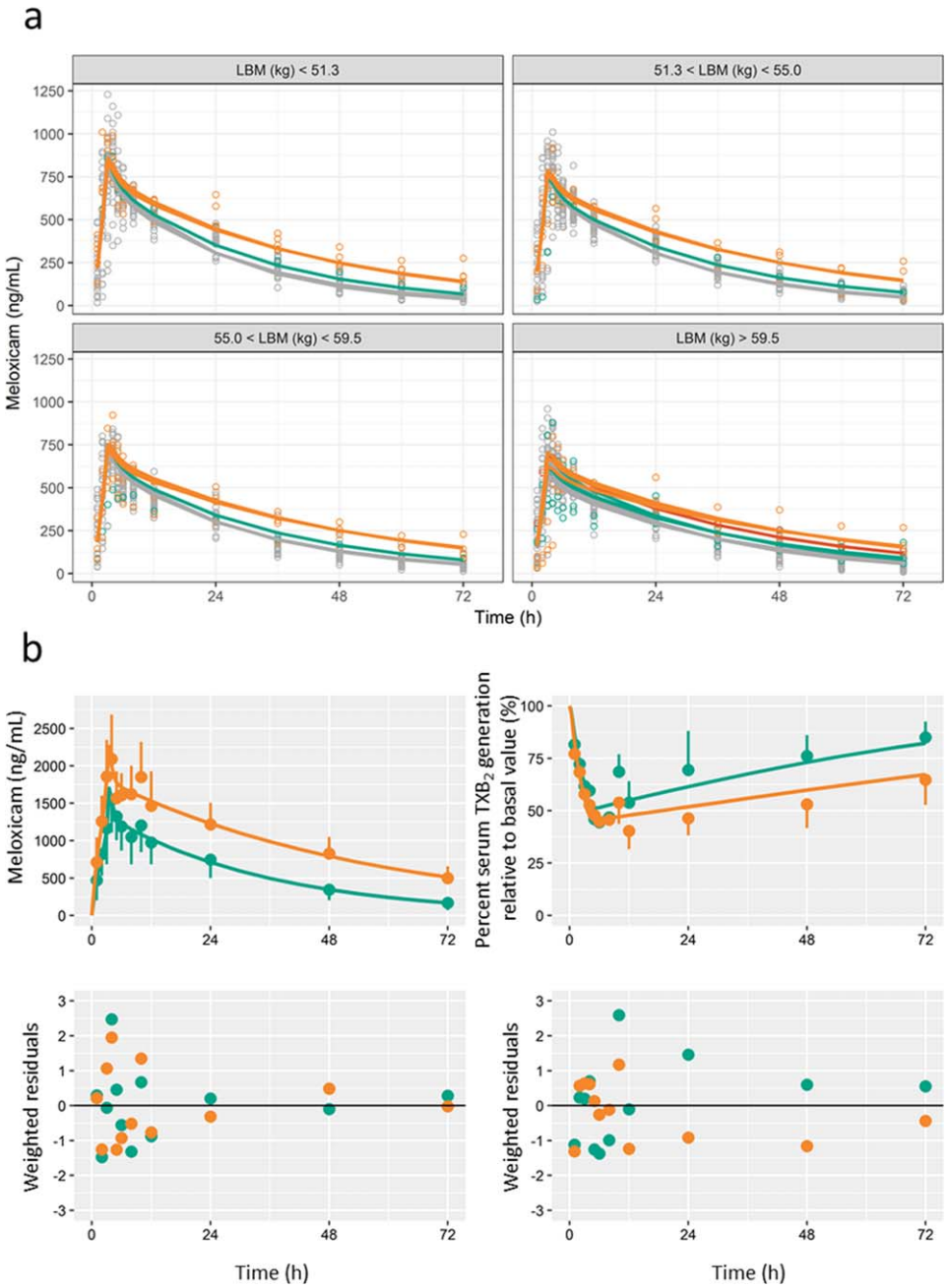


**Figure 3** Graphical fit of the population pharmacokinetic (PK) model and the PK/pharmacodynamic (PD) model. (**a**) Plasma concentration-time profiles of meloxicam stratified by lean body mass; circles represent observed data from Hasunuma *et al.*[6]; lines represent population predictions; colors represent *CYP2C9* genotypes; gray, **1/*1*; green, **1/*2*; orange, **1/*3*; and red, **2/*2*. (**b**) Plasma meloxicam concentration and percent serum thromboxane $B_2$ ($TXB_2$) generation relative to basal value-time profiles; left upper panel, plasma concentration profile after administration of 15 mg of meloxicam; right upper panel, profiles for percent serum $TXB_2$ generation relative to the basal value; left and right lower panel, PK and PD residuals plots. Plasma meloxicam concentration plots represent data from Bae *et al.*,[14] and plots of percent serum $TXB_2$ generation were calculated as the difference between 100% and the scanned percent inhibition of $TXB_2$ generation. Circles represent observed average data. Lines represent predictions. Colors represent *CYP2C9* genotypes; green, **1/*1*; and orange, **1/*13*. Error bars represent SDs. The SDs at 1–8 hours after administration were not digitized because the error bars were not recognized for all groups.

hampered by convergence. Specifically, we observed fluctuating plasma concentration profiles during the elimination phase in white subjects (**Figure 1a**) but observed little or no fluctuations among East Asian subjects. In the enterohepatic circulation model, plasma concentration data for the second and third peaks of the elimination phase and reabsorption processes are required. However, because blood sampling was performed every 12 hours during the

**Table 3** Parameter estimates for the pharmacokinetic/pharmacodynamic model

| Parameter | *CYP2C9*1/*1* Estimate (%RSE) | | *CYP2C9*1/*13* Estimate (%RSE) |
|---|---|---|---|
| CL (L/h) | 0.320 (1.35) | | 0.147 (2.12) |
| Vc (L) | 5.24 (6.35) | | 3.38 (22.9) |
| Q (L/h) | 3.41 (18.5) | | 3.38 (22.4) |
| Vp (L) | 5.18 (6.89) | | 4.55 (20.4) |
| $k_a$ (/h) | 5.01 (9.18) | | 5.27 (8.48) |
| DT (h) | 2.99 (0.140) | | 2.96 (0.242) |
| F | 0.653 (2.25) | | 0.713 (8.79) |
| $k_{out}$ (/h) | | 0.912 (17.2) | |
| $\gamma$ | | 0.739 (9.62) | |
| $IC_{50}$ (ng/mL) | | 1390 (10.2) | |
| $t_{lag}$ = DT, $k_{in} = 100*k_{out}$ | | | |

CL, apparent clearance; DT, duration for meloxicam to enter the central compartment from the absorption compartment by zero-order rate; F, fraction of the dose absorbed by zero-order absorption; $IC_{50}$, plasma meloxicam concentrations that decrease $k_{in}$ by 50%; $k_a$, first-order absorption rate constant; $k_{out}$, first-order rate constant for the decrease in percent serum thromboxane $B_2$ relative to the basal value; Q, apparent intercompartmental clearance; Vc, apparent volume of distribution in the central compartment; Vp, apparent volume of distribution in the peripheral compartment; $\gamma$, sigmoidicity parameter.

elimination phase, reabsorption processes in enterohepatic circulation were not detected. The fluctuation of conditional weighted residuals after 12 hours may be improved by incorporating the enterohepatic circulation model (**Supplementary Figure S1c**). Hence, further studies are required to collect data after intravenous administration and at multiple time points during the elimination phase to describe enterohepatic circulation. Moreover, to describe the second peak or delayed absorption in terms of reabsorption after first-pass effect, we tested a zero-order and first-order parallel absorption with lag time model[39] (**Figure 1b**). In these computations, subjects had convex downward curves or straight lines during the absorption phase, and these interindividual differences were described by the interindividual variability of F.

*CYP2C9* genotypes and LBMs were statistically significant predictors of CL and Vc, respectively, and similarly decreased clearance in carriers of *CYP2C9*2* and/or **3* mutations has been demonstrated for many other drugs. In particular, previous population PK analyses indicated that phenobarbital clearance was decreased by 48% in a Japanese cohort of *CYP2C9*1/*3* carriers,[40] whereas glimepiride clearance was reportedly decreased by 38% in a Korean cohort of subjects with the *CYP2C9*1/*3* genotype.[41] In consistent comparisons with CL in patients with the *CYP2C9*1/*1* genotype, Lane *et al.*[42] showed that (S)-warfarin clearance was decreased by 15%, 33%, 55%, 50%, and 71% in subjects with *CYP2C9*1/*2*, **2/*2*, **1/*3*, **2/*3*, and **3/*3* genotypes, respectively. Hence, decreased clearance ratios in carriers of *CYP2C9*2* and/or **3* mutations are similar for both drugs. These data can also be extrapolated to other drugs that are mainly metabolized by hepatic CYP2C9 and have low hepatic extraction ratios. In addition, Meineke & Türck[7] reported that body weights and

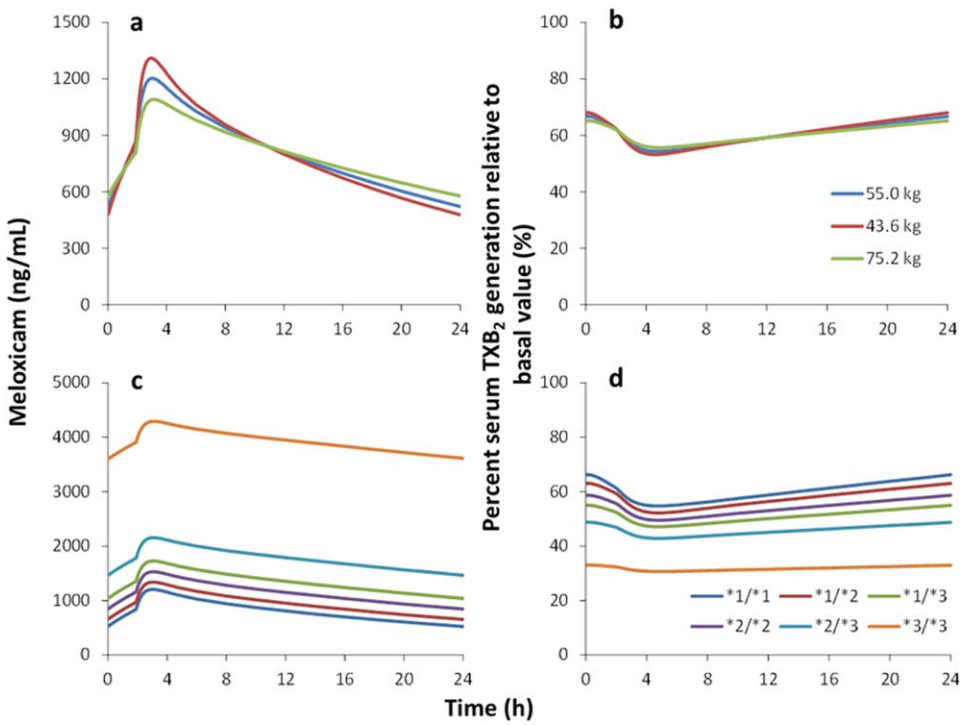


**Figure 4** Relationships between changes in covariates and the effects of meloxicam. The graphs show the impacts of lean body mass (**a, b**) and *CYP2C9* genotypes (**c, d**) on plasma meloxicam concentrations and percent serum thromboxane $B_2$ ($TXB_2$) generation relative to basal value-time profiles. The simulation was performed by varying *CYP2C9* genotypes or lean body mass for 7.5-mg daily meloxicam administration under steady-state conditions. **a** and **b**, *CYP2C9 *1/**1 genotype; **c** and **d**, the lean body mass is 55.0 kg.

age influence the CL of meloxicam, and that body weights affected the volume of distribution of meloxicam in patients with rheumatoid arthritis. However, neither body weights nor ages were statistically significant covariates for CL in the present study, whereas *CYP2C9* genotype was a strong predictor of the CL of meloxicam. Potentially, the influences of body weight and age on CL were obscured by the narrow ranges of these variables herein. However, LBM was a significant covariate for Vc in this study, as shown in patients with rheumatoid arthritis. Moreover, because body size indexes may reflect distributions of meloxicam in extracellular fluid, they were considered a contributor to interindividual variability of Vc, which was reportedly 10.7 L in a noncompartmental analysis.[9]

To simulate the influence of covariates on drug effects, data were retrieved from Bae *et al.*[14] and used to build a PK/PD model for meloxicam. The estimated meloxicam $IC_{50}$ value (1,390 ng/mL shown in **Table 3**) is similar to that (1,100 ng/mL) in a previous study of cyclooxygenase-1 inhibition in whole human blood.[43] Thus, using these data, we applied the PK/PD model (the PD factors) and the final population PK model to evaluate the impacts by *CYP2C9* genotypes and LBM on PD value-time profiles (percent serum $TXB_2$ generation relative to the basal value) for 7.5 mg/day meloxicam administration. Rinder *et al.*[44] showed that the relative serum $TXB_2$ generation was decreased by 37% from baseline at 6 hours after 7.5-mg/day meloxicam administrations under steady-state conditions, but did not evaluate *CYP2C9* genotypes. Thus, we compared this value in simulations of *CYP2C9*1/*1* and **1/*2*, which are common in white populations. In agreement with Rinder *et al.*,[44] our model of subjects with a mean LBM of 55 kg indicated that relative serum $TXB_2$ generation was decreased by 45% and 47% because of *CYP2C9*1/*1* and *CYP2C9*1/*2* genotypes, respectively (**Figure 4d**). Overall, the impact of LBM on the changes in $TXB_2$ generation (**Figure 4b**) were small because changes in meloxicam concentrations varied little with LBM (**Figure 4a**) and the estimated sigmoidicity parameter was 0.739 in the PD model. Therefore, no dosage adjustment was needed on the basis of LBM, which was considered a statistically significant predictor of Vc. We also predicted that the impact of the *CYP2C9*3/*3* genotype was greater than that of the other genotypes, and the time-weighted average relative serum $TXB_2$ generation in carriers of *CYP2C9*3/*3* was 0.53-fold that of *CYP2C9*1/*1* carriers. Hence, analgesic effects of meloxicam are likely stronger among patients with *CYP2C9*3/*3* genotypes, warranting consideration of the risk of gastroduodenal injury in *CYP2C9*3/*3* patients.

The present study is limited primarily by the absence of covariates in the PD models, reflecting the computational availability of average profile data only in published PK/PD studies.[14] However, in a study by Rohatagi *et al.*,[18] no statistically significant covariates for PD parameters of the cyclooxygenase inhibitor CS-706 were detected in population PK/PD analyses. Because meloxicam and CS-706 have similar modes of action, covariates of the PD of meloxicam may also be undetectable.

Finally, only one of the present subjects carried the rare allele combination *CYP2C9*2/*2* genotype. Thus, we modeled *CYP2C9* polymorphisms with assumptions of proportional effects for the subjects with rare allele combinations, as shown in Eq. 5. This proportional effect model has been used in several population PK analyses, including those for dextromethorphan,[28] tolbutamide,[29] and warfarin.[30] However, the present calculated CL value of 0.0782 L/h in subjects with *CYP2C9*3/*3* is greater than the meloxicam oral clearance of $0.043 \pm 0.004$ L/h, which was calculated using a noncompartmental analysis of Korean subjects (mean $\pm$ SD; $n = 3$) with the *CYP2C9*3/*3* genotype,[45] further indicating a comparatively large impact of the *CYP2C9*3/*3* genotype. Thus, further studies are necessary to investigate the PK of rare allele combinations.

In conclusion, we constructed a population PK model using data from our previously published clinical trial data with a single lot of drug, with matched food calories and nutritional contents, and plasma meloxicam concentration measurements that were performed at the same site. No statistically significant ethnic differences in these PK parameters were identified using population analysis, thus expanding the data reported by Hasunuma *et al.*[6] Although the present population PK model showed that *CYP2C9* genotypes and LBM are statistically significant predictors of CL and Vc, respectively, among the factors found in population PK analysis, only *CYP2C9* genotypes affected the PDs of meloxicam during our simulations. Moreover, the effects of the *CYP2C9*3/*3* genotype were larger than those of the other genotypes, warranting careful consideration of the potential for adverse effects in *CYP2C9*3/*3* patients. Finally, the present simulations provided important information for future clinical trials in East Asians with similar genetic backgrounds.

**Acknowledgments.** This study was supported by the Research on Regulatory Science of Pharmaceuticals and Medical Devices from the Japan Agency for Medical Research and Development (AMED). The authors thank Daisuke Suzuki and Tomomi Ogino for their assistance.

**Conflict of Interest.** The authors have no conflicts of interest that are directly relevant to the contents of this research article.

**Author Contributions.** T.A., A.M., and Y.M. wrote the manuscript. M.T. and S.K. designed research. M.T. and Y.S. performed the research. T.A., Y.I., M.K., and Y.M. analyzed the data.

1. Mori, K. & Toyoshima, S. Recent approaches by the PMDA to promoting new drug development: change in the status of the PMDA in relation to new drug development over the last five years. *Drug Inf. J.* **43**, 47–55 (2009).
2. Fukunaga, S., Kusama, M., Arnold, F.L. & Ono, S. Ethnic differences in pharmacokinetics in new drug applications and approved doses in Japan. *J. Clin. Pharmacol.* **51**, 1237–1240 (2011).
3. Nakajima, M., Kuroiwa, Y. & Yokoi, T. Interindividual differences in nicotine metabolism and genetic polymorphisms of human CYP2A6. *Drug Metab. Rev.* **34**, 865–877 (2002).
4. Birmingham, B.K. *et al.* Rosuvastatin pharmacokinetics and pharmacogenetics in Caucasian and Asian subjects residing in the United States. *Eur. J. Clin. Pharmacol.* **71**, 329–340 (2015).
5. International Agency for Research on Cancer, GLOBOCAN 2012: estimated cancer incidence, mortality and prevalence worldwide in 2012. <http://globocan.iarc.fr/Pages/fact_sheets_cancer.aspx#> (2012). Accessed 20 July 2017.
6. Hasunuma, T. *et al.* Absence of ethnic differences in the pharmacokinetics of moxifloxacin, simvastatin, and meloxicam among three East Asian populations and Caucasians. *Br. J. Clin. Pharmacol.* **81**, 1078–1090 (2016).

7. Meineke, I. & Türck, D. Population pharmacokinetic analysis of meloxicam in rheumatoid arthritis patients. *Br. J. Clin. Pharmacol.* **55**, 32–38 (2003).
8. Aoki, T. *et al*. Premedication with cyclooxygenase-2 inhibitor meloxicam reduced postoperative pain in patients after oral surgery. *Int. J. Oral Maxillofac. Surg.* **35**, 613–617 (2006).
9. Türck, D., Busch, U., Heinzel, G. & Narjes, H. Clinical pharmacokinetics of meloxicam. *Arzneimittelforschung* **47**, 253–258 (1997).
10. Türck, D., Roth, W. & Busch, U. A review of the clinical pharmacokinetics of meloxicam. *Br. J. Rheumatol.* **35** Suppl 1, 13–16 (1996).
11. Schmid, J., Busch, U., Heinzel, G., Bozler, G., Kaschke, S. & Kummer, M. Pharmacokinetics and metabolic pattern after intravenous infusion and oral administration to healthy subjects. *Drug Metab. Dispos.* **23**, 1206–1213 (1995).
12. Busch, U., Heinzel, G. & Narjes, H. The effect of cholestyramine on the pharmacokinetics of meloxicam, a new non-steroidal anti-inflammatory drug (NSAID), in man. *Eur. J. Clin. Pharmacol.* **48**, 269–272 (1995).
13. Lehr, T., Staab, A., Tillmann, C., Trommeshauser, D., Schaefer, H.G. & Kloft, C. A quantitative enterohepatic circulation model: development and evaluation with tesofensine and meloxicam. *Clin. Pharmacokinet.* **48**, 529–542 (2009).
14. Bae, J.W., Choi, C.I., Jang, C.G. & Lee, S.Y. Effects of CYP2C9*1/*13 on the pharmacokinetics and pharmacodynamics of meloxicam. *Br. J. Clin. Pharmacol.* **71**, 550–555 (2011).
15. Perini, J.A., Vianna-Jorge, R., Brogliato, A.R. & Suarez-Kurtz, G. Influence of CYP2C9 genotypes on the pharmacokinetics and pharmacodynamics of piroxicam. *Clin. Pharmacol. Ther.* **78**, 362–369 (2005).
16. Riendeau, D. *et al*. Biochemical and pharmacological profile of a tetrasubstituted furanone as a highly selective COX-2 inhibitor. *Br. J. Pharmacol.* **121**, 105–117 (1997).
17. Tegeder, I., Lötsch, J., Krebs, S., Muth-Selbach, U., Brune, K. & Geisslinger, G. Comparison of inhibitory effects of meloxicam and diclofenac on human thromboxane biosynthesis after single doses and at steady state. *Clin. Pharmacol. Ther.* **65**, 533–544 (1999).
18. Rohatagi, S. *et al*. Predictive population pharmacokinetic/pharmacodynamic model for a novel COX-2 inhibitor. *J. Clin. Pharmacol.* **47**, 358–370 (2007).
19. Beal, S.L., Sheiner, L.B. & Boeckmann, A.J. eds. NONMEM Users Guide (1989–2011). (Icon Development Solutions, Ellicott City, MD, 2011).
20. Lindbom, L., Pihlgren, P. & Jonsson, E.N. PsN-Toolkit–a collection of computer intensive statistical methods for non-linear mixed effect modeling using NONMEM. *Comput. Methods Programs Biomed.* **79**, 241–257 (2005).
21. Jonsson, E.N. & Karlsson, M.O. Xpose–an S-PLUS based population pharmacokinetic/pharmacodynamic model building aid for NONMEM. *Comput. Methods Programs Biomed*. **58**, 51–64 (1999).
22. Nguyen, T.H. *et al*. Model evaluation of continuous data pharmacometric models: metrics and graphics. *CPT Pharmacometrics Syst. Pharmacol.* **6**, 87–109 (2017).
23. Bouzom, F., Laveille, C., Merdjan, H. & Jochemsen, R. Use of nonlinear mixed effect modeling for the meta-analysis of preclinical pharmacokinetic data: application to S 20342 in the rat. *J. Pharm. Sci.* **89**, 603–613 (2000).
24. Green, B. & Duffull, S.B. What is the best size descriptor to use for pharmacokinetic studies in the obese? *Br. J. Clin. Pharmacol.* **58**, 119–133 (2004).
25. Imai, E., Yasuda, Y. & Makino, H. Japan Association of Chronic Kidney Disease Initiatives (J-CKDI). *JMAJ* **54**, 403–405 (2011).
26. Ma, Y.C. *et al*. Modified glomerular filtration rate estimating equation for Chinese patients with chronic kidney disease. *J. Am. Soc. Nephrol.* **17**, 2937–2944 (2006).
27. Lee C.S. *et al*. Ethnic coefficients for glomerular filtration rate estimation by the Modification of Diet in Renal Disease study equations in the Korean population. *J. Korean Med. Sci.* **25**, 1616–1625 (2010).
28. Abduljalil, K. *et al*. Assessment of activity levels for CYP2D6*1, CYP2D6*2, and CYP2D6*41 genes by population pharmacokinetics of dextromethorphan. *Clin. Pharmacol. Ther.* **88**, 643–651 (2010).
29. Kirchheiner, J. *et al*. Impact of CYP2C9 and CYP2C19 polymorphisms on tolbutamide kinetics and the insulin and glucose response in healthy volunteers. *Pharmacogenetics* **12**, 101–109 (2002).
30. Hamberg, A.K. *et al*. A pharmacometric model describing the relationship between warfarin dose and INR response with respect to variations in CYP2C9, VKORC1, and age. *Clin. Pharmacol. Ther.* **87**, 727–734 (2010).
31. Bergstrand, M., Hooker, A.C., Wallin, J.E. & Karlsson, M.O. Prediction-corrected visual predictive checks for diagnosing nonlinear mixed-effects models. *AAPS J.* **13**, 143–151 (2011).
32. Lindauer, A. *et al*. Pharmacokinetic/pharmacodynamic modeling of biomarker response to sunitinib in healthy volunteers. *Clin. Pharmacol. Ther.* **87**, 601–608 (2010).
33. "Interview form" of Morbic® Tablets. <http://www.info.pmda.go.jp/go/interview/1/650168_1149035F1020_1_118_1F.pdf> (2011). Accessed 31 October 2013.
34. Aoyama, T. *et al*. Pharmacokinetic/pharmacodynamic modeling and simulation of rosuvastatin using an extension of the indirect response model by incorporating a circadian rhythm. *Biol. Pharm. Bull.* **33**, 1082–1087 (2010).
35. Matsumoto, Y. *et al*. Population pharmacokinetic-pharmacodynamic modeling of TF-505 using extension of indirect response model by incorporating a circadian rhythm in healthy volunteers. *Biol. Pharm. Bull.* **28**, 1455–1461 (2005).
36. Rose, R.H., Neuhoff, S., Abduljalil, K., Chetty, M., Rostami-Hodjegan, A. & Jamei, M. Application of a physiologically based pharmacokinetic model to predict OATP1B1-related variability in pharmacodynamics of rosuvastatin. *CPT Pharmacometrics Syst. Pharmacol.* **3**, e124 (2014).
37. Ide, T., Sasaki, T., Maeda, K., Higuchi, S., Sugiyama, Y. & Ieiri, I. Quantitative population pharmacokinetic analysis of pravastatin using an enterohepatic circulation model combined with pharmacogenomic information on SLCO1B1 and ABCC2 polymorphisms. *J. Clin. Pharmacol.* **49**, 1309–1317 (2009).
38. Savic, R.M., Jonker, D.M., Kerbusch, T. & Karlsson, M.O. Implementation of a transit compartment model for describing drug absorption in pharmacokinetic studies. *J. Pharmacokinet. Pharmacodyn.* **34**, 711–726 (2007).
39. Abe, S., Chiba, K. & Suwa, T. Low-molecular-weight heparin pharmacokinetics: a dual absorption model approach. *Int. J. Clin. Pharmacol. Ther.* **51**, 482–489 (2013).
40. Goto, S. *et al*. Population estimation of the effects of cytochrome P450 2C9 and 2C19 polymorphisms on phenobarbital clearance in Japanese. *Ther. Drug Monit.* **29**, 118–121 (2007).
41. Yoo, H.D., Kim, M.S., Cho, H.Y. & Lee, Y.B. Population pharmacokinetic analysis of glimepiride with CYP2C9 genetic polymorphism in healthy Korean subjects. *Eur. J. Clin. Pharmacol.* **67**, 889–898 (2011).
42. Lane, S. *et al*. The population pharmacokinetics of R- and S-warfarin: effect of genetic and clinical factors. *Br. J. Clin. Pharmacol.* **73**, 66–76 (2012).
43. van Haeringen, N.J., van Sorge, A.A., Van Delft, J.L. & Carballosa Coré-Bodelier, V.M. Flurbiprofen and enantiomers in ophthalmic solution tested as inhibitors of prostanoid synthesis in human blood. *J. Ocul. Pharmacol. Ther.* **16**, 345–352 (2000).
44. Rinder, H.M., Tracey, J.B., Souhrada, M., Wang, C., Gagnier, R.P. & Wood, C.C. Effects of meloxicam on platelet function in healthy adults: a randomized, double-blind, placebo-controlled trial. *J. Clin. Pharmacol.* **42**, 881–886 (2002).
45. Lee, H.I. *et al*. Strongly increased exposure of meloxicam in CYP2C9*3/*3 individuals. *Pharmacogenet. Genomics* **24**, 113–117 (2014).



Supplementary information accompanies this paper on the *CPT: Pharmacometrics & Systems Pharmacology* website (http://psp-journal.com)